EELS measurements in single wall Boron Nitride nanotubes

R. Arenal, O. Stephan, M. Kociak, D. Taverna, C. Colliex et al.

Citation: AIP Conf. Proc. **723**, 293 (2004); doi: 10.1063/1.1812093
View online: http://dx.doi.org/10.1063/1.1812093
View Table of Contents: http://proceedings.aip.org/dbt/dbt.jsp?KEY=APCPCS&Volume=723&Issue=1
Published by the American Institute of Physics.

EELS measurements in single wall Boron Nitride nanotubes

R. Arenal[1], O. Stephan[2], M. Kociak[2], D. Taverna[2], C. Colliex[2], A. Rubio[3], A. Loiseau[1]

[1] LEM, Onera-Cnrs, 29 Avenue de la Division Leclerc, BP 72, 92322 Châtillon, France
[2] Laboratoire de Physique Solides, Université Paris-Sud, 91405 Orsay, France
[3] Dpto. Fisica de Materiales, UPV-DIPC, 20018 San Sebastian, Spain

Abstract. We present here the results of an electron energy loss spectroscopy (EELS) study in scanning transmission electron microscopy (STEM) on boron nitride nanotubes (BN-NTs). The low and core-loss regions have been analyzed to provide by the same technique a combined information about chemical bonding in the different materials in the sample and the electronic properties of individual BN-NTs. In particular, we deduce an optical gap value of about 5.8 eV for single walled nanotubes, which is independent on diameter.

INTRODUCTION

Carbon nanotubes have been the subject of an enormous number of studies concerning their synthesis, electronic, mechanics, optical properties… Although carbon nanotubes were the first to be discovered and remain the most well-known, they are not the unique form. Boron nitride nanotubes are an attractive alternative to carbon. They possess the same hexagonal structure, with boron and nitrogen atoms on alternate lattice sites. The result is a highly polar dielectric material, with a predicted wide band gap close to 5.5 eV, which is supposed to be independent on the tube diameter and helicity [1].

In the work reported here, we have used Transmission Electron Microscopy (TEM) imaging in combination with dedicated Scanning Transmission Electron Microscopy (STEM) experiments to investigate the chemical composition and electronic properties of the BN-NTs.

EXPERIMENT

BN-Nts were synthesized using a laser vaporization technique as described elsewhere [2].

The collected raw powder is dissolved in ethanol and ultrasonically dispersed. A drop of the solution is placed on a copper grid covered by a holey carbon film for electron microscopy study.

TEM images were performed using a Philips CM20 (at 200KV) microscope. The EELS measurements were carried out in a STEM VG-HB501 operated a 100 kV. It is

CP723, *Electronic Properties of Synthetic Nanostructures,* edited by H. Kuzmany et al.

equipped with a cold field emission source (CFE), and a Gatan 666 parallel- EELS spectrometer. EEL spectra were recorded with a charge-coupled device camera optically coupled to a scintillator in the image plane of a Gatan magnetic sector. The high brightness CFE source allows the formation of small probes (0,5 nm) containing a primary current of 0.1 nA and with an energy spread of 0.3-0.4 eV. That provides appropriate conditions to record a spectroscopic information at the nanometer scale on individual nanostructures in the Spectrum-imaging mode. This mode consists of the acquisition of one EEL spectrum for each position of the probe. As the probe scans over a 2D region of the sample, then, it is possible to obtain not only the data to be analyzed but also the spatial statistics of a collection of spectra to be exploited.

RESULTS AND DISCUSSION

Description of the samples

The samples display a relatively heterogeneous morphology [3]. In figure 1 which shows a general view of the samples, it is possible to distinguish NTs (isolated or in bundles) and particles of various sizes and shapes. The NT diameter distribution is centered at 1.4 nm (FWHM=0.6 nm) and 1.6 nm (FWHM=0.3 nm) for isolated tubes or bundles, respectively. The bonding state and chemical composition of the individual nanostructures were determined by EELS. Tubes were found to be made of sp^2 bonded BN with a boron to nitrogen ratio equal to unity. Within the detection and resolution limit of the detector, no carbon was detected to be in substitution to either boron or nitrogen. The particles are in general of pure boron. The surface of a few of them is enriched in oxygen forming a thin boron oxide layer and covered by several sheets of h-BN [3,4], as emphasized below.

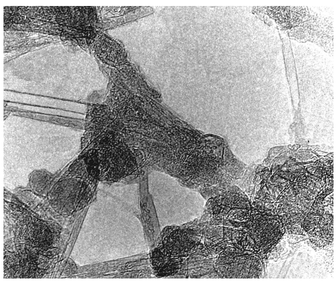

FIGURE 1. High Resolution TEM image, showing bundles and individual NTs and some particles.

Core losses – NNLS fitting

The NNLS (Non Negative Linear Square) fitting method was used to understand the complex situations in our samples. This technique consists of the reconstruction of the experimental EEL spectrum from a linear combination of reference spectra. The NNLS fit was applied only to the B-K edge. The reference spectra (B, B_2O_3, h-BN) were recorded at 0.5 eV dispersion and the fitting window considered was about 30 eV to distinguish the differences between electronic states in the different B compounds. Chemical maps can be obtained from the weights associated to the different references in the total reconstructed spectrum. The example of figure 2 illustrates the structure of a set of boron particles covered by a boron oxide layer and encapsulated in h-BN cages.

h-BN is an anisotropic layered material. The fine structures in B-K edge depend strongly on the orientation of the scattering vector with respect to the lattice. These effects are shown in figure 2 (d) and e)). The NNLS maps were obtained for two references of h-BN, which correspond to the two extreme orientation situations [4].

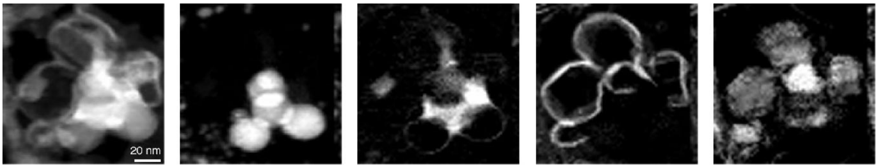

FIGURE 2. a) High Annular Dark Field image, showing a cluster of h-BN cages. b), c), d), e) NNLS maps for pure Boron, boron oxide and h-BN for the 2 orientations (edge and center), respectively.

Low losses

We next turn to the low-loss region study. In this energy region, the physical phenomena involve excitations of valence electrons (collective plasma oscillations and/or interband transitions), which define the structure of the band gap in the case of semiconducting or insulating materials. Low-loss EELS spectra were obtained by summing 500 unsaturated spectra acquired on isolated individual NTs with a dwell time of 40 ms. In order to disentangle the inelastic signal at low energy from the tail of the zero-loss peak (ZLP), a deconvolution procedure based on a Richardson-Lucy algorithm [5] was applied in combination with a subtraction operation of the ZLP. This spectroscopic information was combined with a structural one (diameter and number of layers) deduced from a bright field image systematically acquired on the investigated individual nano-object. Some processed spectra acquired on individual SWNTs of various diameters are displayed on the left of figure3. Such spectra contain the signature of surface modes excited in a near-field geometry where the electron beam is focussed at a grazing incidence of the nano-object and does not intersect with it. In this geometry and for a SWNT, it has been shown that the energy loss suffered by the incident electron is proportional to the imaginary part of the polarisability (by unit length) and writes as a function of $\mathrm{Im}(\varepsilon_{\perp}) + \mathrm{Im}(-1/\varepsilon_{//})$ where $\varepsilon_{\perp}$ and $\varepsilon_{//}$ are respectively the in-plane and out-of-plane components of the dielectric tensor of a planar h-BN sheet [6]. All the three spectra display two groups of modes, a first one in the 6-9 eV range and a second one centered at 16 eV. In agreement with the experimental dielectric constants published in [7], these modes can mainly be attributed to the $\mathrm{Im}(\varepsilon_{\perp})$ contribution in the dielectric response of the tubes. The intermediate feature in the 12 eV range is a contribution from $\varepsilon_{//}$. As the onset of the spectrum mainly reflects the contribution of $\mathrm{Im}(\varepsilon_{\perp})$, one can in principle deduce a value for the optical gap of the different investigated NTs. We find an homogeneous value around 5.8 eV [8]. Calculations are currently in process to interpret the slight variations in the lowest excitations modes and in particular the sharp feature at the onset of the spectra as a function of the diameter of the tubes. For comparison, spectra acquired in a penetrating geometry on other types of nano-objects (double and triple wall nanotubes and ropes) are displayed on the right of figure 3. The main differences with the SWNTs spectra (a higher intensity in the second mode of the doublet at the onset of the spectrum and a small extra intensity above 20 eV) come from extra contributions of volume modes excited in these objects for a penetrating geometry [8].

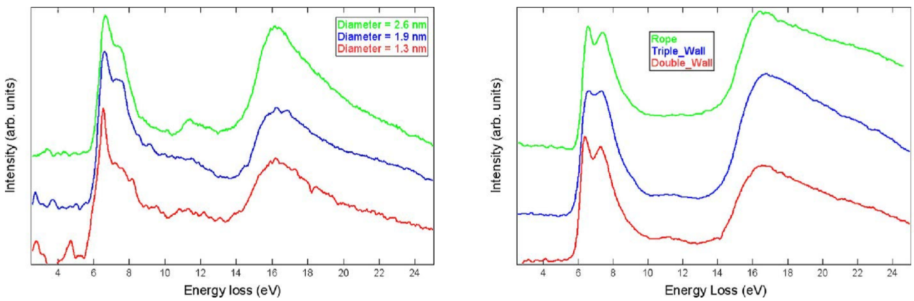

FIGURE 3 Inelastic signal in the low-loss energy region after removal of the zero-loss peak acquired on individual single walled nanotubes (left) and multiwalled and ropes of nanotubes (right).

CONCLUSION

We have presented a combined study of the EELS core and low-loss regions on BN-NTs and Boron nanoparticles. The mapping of the electronic states of boron was performed in order to push the limits of the usual information delivered by conventional chemical mapping. Preliminary results on the optical properties of individual BN-SWNTs were obtained, indicating an homogeneous optical gap value as a function of the tube diameter of about 5.8 eV.

ACKNOWLEDGMENTS

This work has supported by a TMR contract COMELCAN (HPRN-CT-2000-00128).

REFERENCES

1 X. Blase, A. Rubio, S.G. louie, M.L. Cohen *Europhys. Lett*. **28**, 335 (1994).
2 R. S. Lee, J. Gavillet, M. Lamy de la Chapelle, A. Loiseau, J.-L. Cochon, D. Pigache, J. Thibault, F. Willaime, *Phys. Rev. B* **64**, 121405 (2001).
3 R. Arenal, O. Stephan, J.Y. Mevellec, S. Lefrant, A. Rubio, A. Loiseau, submitted 2004.
4 O. Stephan, A. Vlandas, R. Arenal de la Concha, A. Loiseau, S. Trasobares, C. Colliex, EMAG conference Proceedings (2003) and R. Arenal, O. Stephan, A. Loiseau, (to be published).

5 A. Gloter, A; Douiri, M. Tencé, C. Colliex, *Ultramicroscopy* **96**, 385 (2003).
6 O. Stephan, D. Taverna, M. Kociak, K. Suenaga, L. Henrard, C. Colliex, *Phys. Rev. B* **66**, 155422 (2002).
7 G. G. Fuentes, E. Borowiak-Palen, T. Pichler, X. Liu, A. Graff, G. Behr, R. J. Kalenczuk, M. Knupfer, *Phys. Rev. B* **67**, 35429 (2003).
8 R. Arenal, O. Stephan, D. Taverna, M. Kociak, A. Rubio, C. Colliex, A. Loiseau, (to be published).